Scilight

Applied Mathematics and Statistics
https://www.sciltp.com/journals/ams

Check for updates

Article

Energy-Efficient Power Allocation for Cell-Free Massive MIMO Systems

Ebenezer Baidoo Bediako [1,*], Kusi Ankrah Bonsu [2], Kwaku Fokuoh Darkwah [1], John Amoah-Mensah [3], Joseph Wumboranaan Nanjo [2,4] and Kwame Oteng Gyasi [4]

[1] Department of Mathematics, Kwame Nkrumah University of Science and Technology (KNUST), Kumasi 00233, Ghana
[2] Department of Electrical and Electronic Engineering, Sunyani Technical University, Sunyani P.O. Box 206, Ghana
[3] Department of Computer Science, Sunyani Technical University, Sunyani P.O. Box 206, Ghana
[4] Department of Telecommunication Engineering, Kwame Nkrumah University of Science and Technology (KNUST), Kumasi 00233, Ghana
* Correspondence: ebenezerbediako30@gmail.com

How To Cite: Bediako, E.B.; Bonsu, K.A.; Darkwah, K.F.; et al. Energy-Efficient Power Allocation for Cell-Free Massive MIMO Systems. *Applied Mathematics and Statistics* **2026**, *3*(2), 11. https://doi.org/10.53941/ams.2026.100011

Received: 23 March 2026
Revised: 28 May 2026
Accepted: 12 June 2026
Published: 8 July 2026

Abstract: The study investigates a power allocation model for cell-free massive Multiple Input Multiple Output (CF-mMIMO) systems using the Accelerated Proximal Gradient (APG) algorithm.CF- mMIMO systems are a crucial component of sixth-generation networks (6G) that aim to improve system energy efficiency. Unlike conventional optimization approaches that rely on computationally intensive convex relaxation or second-order solvers, the proposed method directly addresses the inherently non-convex fractional energy-efficiency maximization problem under Quality of Service (QoS) and access point (AP) power constraints. A differentiable quadratic penalty mechanism is introduced to seamlessly incorporate the QoS constraints into the objective function, thereby transforming the constrained non-convex problem into a tractable penalized optimization problem suitable for first-order iterative optimization. Validation of the APG algorithm's resilience revealed that it outperformed benchmark algorithms in terms of energy efficiency and execution time, demonstrating its usefulness for challenging optimization tasks, particularly those involving bursty communication. Furthermore, the APG technique guarantees that no penalty functions (PFs) are broken, ensuring that the overall loss converges to zero, irrespective of the beginning conditions.

Keywords: energy efficiency; resource allocation; cell-free massive MIMO and power allocation

1. Introduction

Massive Multiple-Input Multiple-Output (MIMO) technology is necessary for modern wireless communication systems, particularly in light of 5G and upcoming technologies. It involves using a large number of antennas at the base station to serve multiple consumers at once, improving dependability, energy efficiency, and spectrum efficiency.Massive MIMO offers a number of significant benefits and characteristics, such as reduced interference, improved energy efficiency, higher throughput and capacity, and increased reliability [1].

Cell-free massive MIMO is an extension of the massive MIMO concept that attempts to address some of the issues with traditional cellular networks. Instead of having a network divided into distinct cells, cell-free massive MIMO disperses a vast number of distributed access points (APs) over a coverage area, all of which are connected to a central processing unit (CPU). In order to offer the users shared services, the APs collaborate. Numerous advantages come with cell-free massive MIMO, including flexibility, scalability, and the elimination of cell borders as well as continuous service quality [2]. Due to its ability to provide high throughput without necessitating an increase in system bandwidth, the cell free massive Multiple-Input Multiple-Output (MIMO) technique has made tremendous progress [3]. The ultimate paradigm in wireless communication evolution is Cell-Free Massive MIMO systems. These systems also result in better energy efficiency since they may minimize coverage gaps and resolve capacity concerns. The integration of energy-efficient resource allocation with cell-free massive MIMO has the potential to revolutionize the wireless communication landscape [4]. These ideas will inevitably come to pass as long as research projects continue and technology advances, which will determine how wireless communication systems develop going forward [5]. In the rapidly evolving field of wireless communication, the introduction of Cell-free massive MIMO systems holds great promise for resolving capacity and coverage challenges while preserving energy efficiency. On the other hand, power allocation and access point deployment pose major challenges to the effective operation of such systems. The main objective is to take into account the dynamic nature of wireless environments and find a careful balance between maximizing the number of access points and wisely allocating transmit power.

Cell-free massive MIMO systems address the capacity limitations and coverage gaps present in traditional cellular networks by distributing access points (APs). However, there is still disagreement regarding the ideal quantity of APs to install. An excessive number of APs deployed could result in wasteful energy use, expensive equipment, and difficult management. On the other hand, if there are too few APs installed, coverage and capacity improvements may be compromised, and the technology's potential advantages may not be completely realized.

Furthermore, achieving the energy-saving benefits of cell-free Massive MIMO systems depends on effective power distribution. Both interference control and signal quality enhancement must be taken into account when allocating transmit power. While giving some APs too much strength can result in inefficiencies, giving other APs not enough power could worsen user experience. The continual changes in user locations, channel conditions, and interference levels exacerbate this complex optimization challenge.

The authors in [6] and [7] created the best power allocation algorithms for Orthogonal Frequency Division Multiplexing (OFDM) when the channel state information (CSI) was not perfect.

In order to circumvent transmission power constraints and reception interference, the authors in [8] developed quantized power allocation techniques. This made it possible to further optimize system throughput. The authors in [9] suggested an improved method for allocating water filling power that could result in the highest system throughput in an LF scenario. The authors in [10] developed a novel and straightforward expression for the power that optimized the energy efficiency of massive Multiple Input Multiple Output systems without cells. EE power allocation was the subject of [11], where the total transmitted power and the number of users in a cell are closely related.

Ref. [12] examines a resource allocation problem for downlink cell-free massive MIMO networks, where each access point serves a cluster of user equipment. To ensure consistent and excellent service throughout the coverage area, transmit precoding and power allocation are linked to the underlying max-min scheduling. The resulting max-min resource allocation optimization problem is non-convex since user equipment is networked. We prove the uplink-downlink duality and offer a productive iterative method to address the fundamental downlink issue. By using the max-min beam former and accounting for the inaccuracy of the channel estimate, we get the capacity lower bound of the underlying cell-free massive MIMO network.

Ref. [13] gave a performance comparison between the scenarios of perfect fronthaul links, the scenario where the CPU has access to the quantized version of the estimated channel and the quantized signal, and the case where the CPU only has access to the quantized weighted signal. The quantization effect is represented using the Bussgang decomposition. The max-min paradox, which optimizes the minimum rate by taking advantage of the fronthaul capacity and power limitations, is the subject of the study. Power allocation problems are addressed using geometric programming (GP), which solves the non-convex problem. An iterative procedure combined with uplink-downlink duality is utilized to show that the proposed method is optimal. Performance is significantly improved by using the suggested user assignment strategy.

A deep neural network (DNN) was presented by Zhao and associates in 2020 as a potential solution to the issue of an accurate max-min power optimization solution requiring excessive time complexity for a given time budget. A DNN has a low execution time complexity, but before it can be used, it needs to undergo a lot of offline training. There are four completely linked layers and two convolutional layers in the suggested CNN. It sends the power of each antenna element to each user based on the input of long-term fading data.

A feasible data rate equation for a multi-user, multiple-input, multiple-output system with little feedback of channel condition information is given by [14]. When there are limitations on quality of service (QoS), power allocation maximizes energy efficiency (EE). Energy-efficient unequal power allocation (EEUPA) with the Lagrange multiplier of the CSI system is supported by mathematical equivalency. It is encouraging for next-generation wireless networks as the data demonstrate that EE grows with transmit antenna count.

The optimization of restricted feedback energy efficiency for MU-MIMO systems is investigated by [15]. The potential data rate for RRH-user selection is calculated, and this yields the energy efficiency (EE) optimization

https://doi.org/10.53941/ams.2026.100011

framework. The system EE is optimized by power allocation, RRH-user selection, and antenna number change when the maximum transmit power constraints and quality of service criteria are satisfied. It is currently NP-hard and non-convex. Using successive convex approximation and Lagrange dual decomposition, a workable solution to the problem is proposed.

Power allocation maximizes energy efficiency when quality of service (QoS) is limited. Mathematical equivalency supports the concept of an energy-efficient unequal power allocation (EEUPA) with a Lagrange multiplier of the CSI system. The results show that EE increases with transmit antenna count, which bodes well for next-generation wireless networks [15].

The entire EE optimization issue is nonconvex, and in the successive convex approximation framework, second-order cone programming (SOCPs) are usually employed to solve it. Due to their extreme complexity, these techniques operate slowly, particularly in large networks with thousands of users and access points (APs). The authors proposed two computationally efficient approaches to overcome the aforementioned difficulty: the proximal gradient (PG) technique and the accelerated proximal gradient (APG) method. Except for the aforementioned connected studies, earlier work in the field of massive MIMO has mostly addressed power control problems using the successive convex approximation technique. According to this idea, a series of convex second-order cone programs (SCOPs) can approximate a non-convex problem. Thus, by applying interior point approaches, these methods solve these convex problems at high processing cost. Ref. [16] provided a scalable solution to the backhaul limitations and computational complexity associated with large-scale issues with cell free massive MIMO.

Power allocation strategies that optimize system performance under diverse limitations have witnessed major developments in the realm of massive MIMO. Several noteworthy contributions have been made by [7] and [6] on algorithms for OFDM with imperfect CSI, Ref. [8] on quantized power allocation approaches to optimize system throughput, and [9] on improved water-filling power allocation methods. Moreover, Ref. [10] provided a simple expression for maximizing energy efficiency in large MIMO systems, and [11] investigated the connection between total transmitted power and cell size. In their studies on resource and power allocation in cell-free massive MIMO networks, Refs. [12] and [13] highlighted the difficulties associated with non-convex optimization issues and suggested iterative techniques to guarantee reliable service. In order to address the temporal complexity of max-min power optimization, Ref. [17] proposed a deep neural network (DNN), which, after considerable offline training, provided a low-execution-time solution. Energy-efficient power allocation with QoS constraints was the focus of works by [15] and [14], which employed mathematical equivalency and successive convex approximation to tackle non-convex problems. These research demonstrated that the number of transmit antennas boosts energy efficiency, a finding that holds promise for next-generation wireless networks. But these techniques frequently have a considerable computational complexity, especially when dealing with big networks. The proximal gradient (PG) and accelerated proximal gradient (APG) approaches, which are more effective than conventional second-order cone programs (SOCPs), were proposed by [18] as a solution to the computational difficulties. Even with these improvements, successive convex approximation methods—which can be laborious and costly to compute—remain a major component of most current work. Scalable answers to backhaul constraints and computational complexity in cell-free massive MIMO were given by [16]. Their method did not, however, completely handle linked variable optimization problems with QoS limitations. The necessity for an effective power allocation plan that meets QoS criteria and improves energy economy in cell-free massive MIMO systems drives this research. Our goal is to identify more effective and computationally efficient ways to optimize the overall energy efficiency of these networks, considering the shortcomings of the existing methods.

While Accelerated Proximal Gradient (APG) and projected-gradient techniques in [18] focused on formulating a mixed integer nonconvex optimization problem under constraints on the per-AP transmit power, Quality of Service rate requirements without explicitly incorporating user-level QoS violations through adaptive penalty-driven formulations, In contrast, the proposed work introduces a penalty-based APG framework tailored for non-convex energy-efficiency maximization in cell-free massive MIMO systems under coupled QoS and AP power constraints.

These papers aim at developing an advanced power allocation strategies (Accelerated Projected Gradient (APG)) algorithm that consider the dynamic network conditions to minimize energy consumption while ensuring high-quality signal delivery, and the proposed algorithm will be use against benchmarked algorithms.

The problem at hand is non-convex, which means it involves optimizing a function with intricate, potentially non-linear constraints. For this reason, the APG approach is selected. APG offers a strong method for solving non-convex problems and is renowned for its efficacy in doing so. Once more, it combines the benefits of proximal and gradient descent techniques, resulting in a faster convergence than classical optimization algorithms. Faster convergence is essential for practical implementation in the massive MIMO systems setting, where many variables are involved.

The following is a summary of the primary contributions made in this paper:

(1) By presenting a revolutionary power distribution model for Cell-Free Massive Multiple Input Multiple Output systems, this research greatly improves the field of sixth-generation networks (6G). Enhancing the system's energy efficiency is the primary objective, as it plays a crucial role in the development of upcoming wireless communication technologies. The suggested model maximizes execution time and energy efficiency by employing an Accelerated Proximal Gradient (APG) technique.

(2) The main innovation of this work lies in the simultaneous handling of user-level Quality of Service (QoS) requirements and transmit power limitations at the Access Points (APs). To achieve this, the study formulates an energy-efficiency maximization problem that is inherently non-convex due to the coupled SINR expressions and fractional objective structure. Instead of solving the constrained non-convex problem directly, a quadratic penalty function is introduced to incorporate the QoS constraints into the objective function by penalizing constraint violations. This transforms the original constrained optimization problem into an equivalent unconstrained penalized optimization framework that is more tractable for iterative first-order optimization methods. This conversion guarantees robustness in the face of dynamic communication settings by facilitating the effective use of the APG algorithm.

(3) The paper thoroughly evaluates the suggested algorithm's performance through a comparative study using benchmark algorithms. The results demonstrate how much better the APG algorithm can operate, particularly with regard to energy efficiency and execution time. This demonstrates the usefulness of the suggested model, indicating that it is a good fit for handling challenging optimization problems in situations involving bursty communication. Essentially, this research makes a substantial contribution to the development of 6G networks by offering a reliable and effective solution for power allocation in CF-mMIMO systems.

Section 2 reviews the relevant works. Section 3 describes the optimization of overall energy efficiency in cell-free massive MIMO. Section 4 presents the suggested APG technique for this optimization. Section 5 includes the simulation results and discussions. The notation table is shown in Table 1.

Table 1. Notation table.

Variables	Definition
τ_p	Pilot length
ρ_p	pilot transmit power
ϕ_k	pilot sequence assigned to k-th user
$g_{mk} \in \mathbb{C}^{L\times 1}$	channel vector between k-th user and m-th AP.
ι_{mk}	Large-scale fading co-efficient
$a_{mk} \sim \mathcal{CN}(0, I_L)$	Small -scale factor vector with independent complex Gausian entries
L	Number of antennas at the AP
$R_{mk} \in \mathbb{C}^{L\times L}$	Spartial correlation matrix between the antennas of the m-th AP for user k
σ_k^2	Scale fading variance
I	Identity matrix
L_m	Transmitted Signal vector from AP m
$\eta_k \sim \mathcal{CN}(0, 1)$	Additive white Gaussian Noise
$SINR_k$	Signal - to- Interference-Plus- Noise Ratio for k-th user
ω_{mk}	Precoding vector
$\hat{g}_{mk}$	estimated channel
λ_{mk}	Power controll coefficient
SE_k	Spectral Efficiency for k-th user
$\omega_k(\Theta)$	QoS violation penalty
χ	Penalty weight

2. System Model

We analyze a large MIMO system without a cell that uses time division duplex (TDD) to function in both downlink and uplink modes (see Figure 1). The *M* access points (APs) and *K* users of this system are dispersed randomly throughout the surroundings. Each AP has one or more *L* antennas, and each user has one antenna. The central processing unit (CPU) and each access point (AP) are connected by a fronthaul connection with a high capacity and no errors. In scenarios based on TDD, three processes are divided into each coherence interval τ_c: uplink data communication, downlink training, and uplink training. Here, we concentrate on both the downlink and uplink training stages.

The remaining coherence interval, $\tau_c - \tau_p$, is set aside for uplink data transfer, assuming an uplink training period of τ_p.

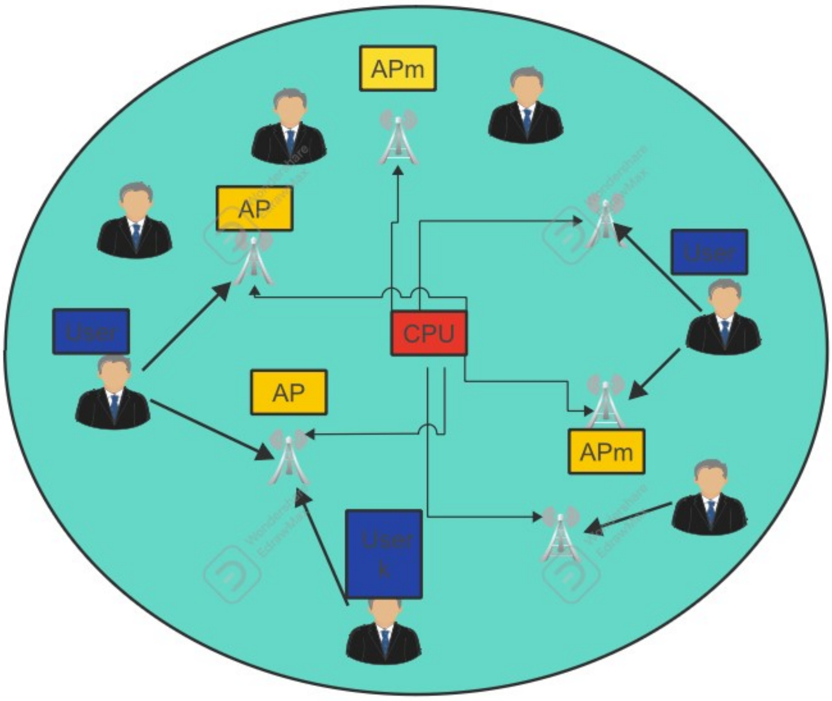

Figure 1. Cell Free Massive MIMO

2.1. Uplink Training Phase

During the training phase, each *K-th* user simultaneously broadcasts their pilot sequence to each AP.

Assume that $\sqrt{\tau_p \rho_p}\phi_k \in \mathbb{C}^{\tau_p \times 1}$ is the pilot sequence of the *K-th* user, where $||\phi_k||^2 = 1$, $k = 1, ...K$. Then, the *m-th* AP recieves

$$Z_m = \sqrt{\tau_p \rho_p} \sum_{k=1}^{K} g_{m,k} \phi_k^H + N_m, \tag{1}$$

where τ_p = the duration of each coherence interval's training phase, and ϕ_K = pilot sequence assigned to the K-th user $\tau_p < \tau_c$

$$\phi_K = \begin{bmatrix} \phi_{K,1} \\ \phi_{K,2} \\ \vdots \\ \phi_{K,\tau_p} \end{bmatrix} \in \mathbb{C}^{\tau_p \times 1}$$

ρ_p = SNR was averaged over all pilot symbols.The Gaussian noise with white color and identically distributed and independent components (i.i.d.) is represented by N_m. The channel vector provided by the link between the *k-th* and *m-th* AP is designated by g_{mk}.

$$g_{mk} = \sqrt{\iota_{mk}} a_{mk}, \tag{2}$$

where

$$g_{mk} \in \mathbb{C}^{L \times 1}$$

denotes the channel vector between the k-th user and the m-th access point (AP), **L** representing the number of antennas at the AP

$$\iota_{mk} = \text{the large-scale fading coefficient,}$$
$$a_{mk} = \text{small scale fading.}$$

Assuming that a_{mk} has *i.i.d.* random variables with $\mathcal{CN}(0, I_L)$, g_{mk} is likewise an identically distributed independent variable (i.i.d). The channel gain vector can now be estimated using the *m-th* AP. $g_{mk} \quad \forall k = 1, \ldots, K$.

$$\mathbb{E}\{g_{mk} g_{mk}^H\} = R\sigma_k^2 I,$$

where, mean = 0.

R is a positive constant scaling factor that determines the overall strength of the channel covariance, σ_k^2 denotes the average power associated with the K-th user channel, and **I** is the identity matrix.
similarly, $N_{p,m}$ is i.id and

$$\mathbb{E}\{N_{p,m} N_{p,m}^H\} = R\sigma_2 I.$$

We then apply MMSE, which is a widely utilized method as described in [19] to estimate g_{mk}. This is given by

$$\hat{g}_{mk} = \mathbb{E}\left\{g_{mk} Z_{mk}^H\right\}\left(\mathbb{E}\{Z_{mk}\hat{z}_{mk}^H\}\right)^{-1} Z_{mk} = c_{mk} Z_{mk} \tag{3}$$

where c_{mk} as observed by [20] is

$$c_{mk} = \frac{\sqrt{\tau_p \rho_p}\iota_{mk}}{\tau_p \rho_p \sum_{k'=1}^{K} \iota_{mk'} |\phi_{k'}^H \phi_k|^2 + 1}, \tag{4}$$

where, $\mathbb{E}\left\{g_{mk} Z_{mk}^H\right\}$ is the cross covariance and $\left(\mathbb{E}\{Z_{mk}\hat{z}_{mk}^H\}\right)^{-1}$ is the covariance.

2.2. Downlink Training Phase

Access Points (APs) use channels selected during the training phase in conjunction with conjugate beamforming techniques to precode symbols for every user during the downlink data transmission phase. The signals that the APs have transmitted are represented by the following vector:

$$L_m = \sqrt{\rho_d} \sum_{k=1}^{K} \sqrt{\lambda_{mk}} b_{mk} q_k, \tag{5}$$

where
b_{mk} = beamforming Vector,
q_k = The sign that was meant for **K-th** user,
where
$\mathbb{E}\,|q_k|^2 = 1, \forall k$,
ρ_d = power constraint at each at *m-th* AP,
λ_{mk} = power control co-efficient between the AP_m and user k.
The transmit signal meets the subsequent power requirement:

$$\mathbb{E}\{||L_m||^2\} \leq \rho_d, \tag{6}$$

The equivalent form of (5) is given as:

$$\sum_{k=1}^{K} \lambda_{mk} \mathbb{E}\{||\hat{b}_{mk}||^2\} \mathbb{E}\{|q_k|^2|\} \leq 1, \tag{7}$$

the *k-th* user receives signals as follows:

$$r_k = \sum_{m=1}^{M} g_{mk}^H L_m + n_k, \tag{8}$$

The additive noise at the *K-th* user is denoted by n_k, where $n_k \sim \mathcal{CN}(0, 1)$.

2.3. Spectral Efficiency

The precoding vector $\hat{b}_{mk}$ is determined using the estimated channels during the uplink training phase.By combining the assumptions of $\{|q_k|^2\} = 1$ and (7) and assuming that $\mathbb{E}\{||\hat{b}_{mk}||^2||\} = 1$, the power constraint at AP *m* in (6) can be simplified as follows:

$$\sum_{k=1}^{K} \lambda_{mk} \leq 1, \tag{9}$$

assuming conjugate beamforming (maximum-ratio transmission) based on imperfect channel state information, the achievable downlink spectral efficiency (SE) for the *k-th* user is as follows:

$$Sek(\lambda_{mk}) = (1 - \frac{\tau_p}{\tau_c}) \log_2(1 + SINR_k), \tag{10}$$

where, $\left(1 - \frac{\tau_p}{\tau_c}\right)$ = pilot overhead factor and we define Signal-to -Interference-plus- Noise- Ratio(SINR) as the measure of the quality of the received signal given as:

$$SINR_k = \frac{\rho_d(L - \tau_p)\left(\sum_{m=1}^{M} \sqrt{\lambda_{mk}\gamma_{mk}}\right)^2}{\rho_d \sum_{m=1}^{M} \sum_{k=1}^{K} (\iota_{mk} - \gamma_{mk})\lambda_{mk} + 1}, \tag{11}$$

where, $L - \tau_p$ represent the effective beamforming gain after accounting for the pilot resources utilized for channel estimation, where **L** is the number of AP antennas τ_c = Duration of every coherence interval, τ_p = length for each coherence interval and $\tau_c > \tau_p$.

2.3.1. Power Consumption

Given is the total amount of energy consumed:

$$P_t = \sum_{m=1}^{M} P_{C,m} + \sum_{m=1}^{M} P_{bh,m}, \tag{12}$$

$P_{C,m}$ = energy consumed at AP *m*.

The amount of electricity used by the backhaul link from the Central Processing Unit to the *m-th* access point is denoted by $P_{bh,m}$.

At this point, the energy used at AP *m*is provided as:

$$P_{C,m} = \frac{1}{\mu_m} \rho_d N_o \left(N \sum_{k=1}^{K} \lambda_{mk}\gamma_{mk}\right) + NP_{tc,m}, \tag{13}$$

where

μ_m = amplified power efficiency and lies in $0 \leq \mu_m \leq 1$,

N_O = Noise power,

$P_{tc,m}$ = The amount of power needed by each antenna's circuitry to function as a *m-th* AP.

The backhaul's power consumption is directly correlated with the sum spectral efficiency, and is used to transport data between the CPU and APs.

$$P_{hb,m} = P_{0,m} + Sek(\lambda_{mk}).P_{bt,m}, \tag{14}$$

$P_{0,m}$ = Constant power usage for each backhaul,

$P_{bt,m}$ = dependent power -traffic.

Putting (13) and (14) into (12), we have:

$$P_t = \rho_d \sum_{m=1}^{M} \frac{1}{\alpha_m} \left(N \sum_{k=1}^{K} \lambda_{mk}\gamma_{mk}\right) + \sum_{m=1}^{M} (NP_{tc,m} + P_{0,m}) + \left(\sum_{m=1}^{M} P_{bt,m}\right) S_e(\lambda_{mk}). \tag{15}$$

2.4. Energy Efficiency

Total energy efficiency can be defined as the ratio of total system throughput to total energy consumption. The overall energy efficiency, given in bits/joules numerically, is

$$E_e(\lambda_{mk}) = \frac{SE}{Power \ \ consumption},$$
$$E_e(\lambda_{mk}) = \frac{\sum_{k=1}^{R} S_{ek}(\lambda_{mk})}{P_t}, \tag{16}$$

where
$E_e(\lambda_{mk})$ = Total energy efficiency,
$S_{ek}(\lambda_{mk})$= spectral efficiency,
p_t= total power consumption.

3. Energy Efficiency Optimization Problem

In this instance, each Access Point (AP) is given the power coefficient (λ_{mk}) to optimize overall energy efficiency while meeting total power and quality of service requirements. The optimization problem is stated as follows, to be more precise:

$$\begin{aligned} &\max_{\lambda_{mk}}, E_e(\{\lambda_{mk}\}) \\ &\text{s.t.} \quad S_{ek}(\{\lambda_{mk}\}) \geq \eta_k, \quad \forall k \\ &\qquad \sum_{k=1}^{K} \lambda_{mk} \leq 1, \quad \forall m \\ &\qquad \lambda_{mk} \geq 0, \quad \forall k, \forall m, \end{aligned} \tag{17}$$

where
η_k = quality of service constraint.
Equation (17)'s optimization problem is comparable to

$$\begin{aligned} &\max_{\lambda_{mk}}, \frac{\sum_{k=1}^{K} S_{ek}(\lambda_{mk})}{P_t} \\ &\text{s.t.} \quad S_{ek}(\{\lambda_{mk}\}) \geq \eta_k, \quad \forall k \\ &\qquad \sum_{k=1}^{K} \lambda_{mk} \leq 1, \quad \forall m \\ &\qquad \lambda_{mk} \geq 0, \quad \forall k, \forall m. \end{aligned} \tag{18}$$

It is noteworthy to notice that this problem's objective function exhibits nonconvex properties. Usually, an iterative approach is used to address such nonconvex problems. This involves gradually approximating the original nonconvex function using a series of convex functions. This approach falls into the category of sequential convex approximation. This method is really further developed in [21], where a series of Second-Order Cone Programs (SOCPs) are used to optimize energy efficiency (EE).

It is imperative to acknowledge that this approach becomes considerably more difficult as the system grows, especially with a rise in the number of users and access points (APs). In large, cell free multiple input multiple output systems with several access points and users, this approach might not be suitable for complex optimization challenges. Before using the Accelerated Proximal Gradient technique to address the optimization problem in equation (18), the equation must be reconstructed, and the objective function's gradient must be confirmed to be Lipschitz continuous. To make computations easier, we accomplish this by including more variables. The following representations display the extra variables:

Let

$$\begin{aligned}\Theta &= \lambda_{mk},\\ u(\Theta) &= \sum_{k=1}^{K} Se_k(\lambda_{mk}),\\ v(\Theta) &= P_t.\end{aligned}$$

Currently, the objective function of (18) can be expressed as follows:

$$\frac{u(\Theta)}{v(\Theta)}, \tag{19}$$

and making the following assumptions:

$$\begin{aligned}\Theta_1^* &= \big(\Theta_{11};\Theta_{12};\ldots;\Theta_{1K}\big),\\ \Theta_2^* &= \big(\Theta_{21};\Theta_{22};\ldots;\Theta_{2K}\big).\end{aligned}$$

where all power control coefficients associated with APm are vectorized as $\Theta = [\Theta_1, \Theta_2; ...; \Theta_m] \in \mathbb{R}_+^{M\times k}$. We can now write (18) as:

$$\begin{aligned}\max_{\Theta\in\mathcal{C}} \quad & \frac{u(\Theta)}{v(\Theta)}\\ \textbf{s.t.} \quad & u(\Theta) \geq S_{ok}, \quad \forall m,\\ & \sum_{k=1}^{K}\Theta_k \leq 1, \quad \forall k,\\ & \Theta_k \geq 0, \quad \forall k.\end{aligned} \tag{20}$$

3.1. Proposed APG Method for EE Optimization

Including Quality of Service (QoS) requirements in Equation (20) is a major challenge for any algorithm trying to solve it. This problem has a creative solution that combines the usage of a punishment system and the Accelerated Proximal Gradient (APG) approach. By adding a penalty parameter and a punishment term to the objective function, the penalty approach is applied to the Quality of Service (QoS) constraint. This modification results in a penalty issue. Next, the updated issue is solved using the Accelerated Projected Gradient (APG) method. Until a predetermined stopping criterion is satisfied, the iterative process is repeated.

3.1.1. The penalty Function

The penalty function is used to transform a constrained optimization problem into an unconstrained optimization problem by incorporating the constraints directly into the objective function.

A quadratic loss function is defined for every Quality of Service (QoS) constraint as follows:

$$\omega_k(\Theta) = [max(0, \eta_k - S_{ek})]^2, \tag{21}$$

where $\eta_k =$ QoS target constraint given a penalty coefficient χ, the penalized objective function for equation (20) can be expressed as:

$$h_\chi(\Theta) = \frac{u(\Theta)}{v(\Theta)} - \chi \sum_{k}^{K} \omega_k(\Theta). \tag{22}$$

It is crucial to emphasize that the previously mentioned regularized objective function is framed within the context of maximization. Furthermore, the prudent choice of the penalty coefficient χ is of significance. Assigning a high value to this parameter ensures feasibility but may introduce numerical instability into the resultant optimization problem. On the other hand, an excessively low value can produce a suboptimal solution or result in convergence at a point that violates the constraints.

In practical implementations, the above challenges are typically addressed by first solving the optimization problem that involves the penalized function with a small value of χ, and then verifying that the halting conditions are satisfied. If not, the value of χ can be raised using $\rho(>1)$. After that, this procedure is repeated until the stopping conditions are satisfied. Using the prior iteration's solution as the starting point for the subsequent one is crucial in this iterative process. With a given χ, the following regularized optimization problem is the major emphasis of the penalty technique.

$$\underset{\Theta \in c}{max} \;\; h_\chi(\Theta). \tag{23}$$

where $\mathcal{C}$ is the feasible set, which is the collection of all optimization vectors satisfying the power and nonnegativity constraints.

$$\mathcal{C} = \Theta \in R_+^{MK} : \sum_{k=1}^{K} \lambda_{mk} \leq 1 \quad \forall m$$

3.1.2. The Penalty- Based APG Method

The objective function $h_\chi(\Theta)$ presented in Equation (23) is a well-behaved function characterized by a Lipschitz continuous gradient and an upper bound. Consequently, the Accelerated Proximal Gradient (APG) method can be efficiently applied to solve it.

The ensuing inequalities verify that inter-user interference and overall power consumption are the main factors limiting total energy efficiency (EE). With an upper constraint, $f(\Theta)$ is likewise a valid function. This constraint covers the entire spectral energy (SE).

$$h_\chi(\Theta) = \frac{\tau_c - \tau_p}{\tau_c}\frac{u(\Theta)}{v(\Theta)} - \chi \sum_{k}^{K} [max(0, h_k(\Theta))]^2 \leq B\frac{\tau_c - \tau_p}{\tau_c}\frac{u(\Theta)}{v(\Theta)} < \infty.$$

Ref. [22] provides evidence for the gradient function $h(\Theta)$'s Lipschitz continuity. We have noted that the issue raised by Equation (23) can be effectively resolved by using the APG approach. The algorithm illustrates the suggested methodology, which combines the APG approach and the penalty method, where Θ_χ represents the best solution to Equation (23). Within the framework of the APG process, as shown in the method, it is important to remember that we traverse the gradient direction in an attempt to maximize and improve the current point's objective. Furthermore, when the relative growth in the objective over the preceding 10 iterations is less than ζ, the APG approach pauses for pragmatic reasons. The gradient $\nabla h_\chi(\Theta)$ computation is surely the main operation required to implement the approach.

For $\nabla h_\chi(\Theta)$, the formula is as follows:

$$\nabla h_\chi(\Theta) = \frac{v(\Theta)\nabla u(\Theta) - u(\Theta)\nabla v(\Theta)}{v(\Theta)^2} - \chi \sum_{k=1}^{K} \nabla\omega_k(\Theta), \tag{24}$$

In the context of a maximization problem, the objective function must have a lower bound.

3.1.3. Proposed APG Algorithm For Solving (23)

(1) **input** :Initial point $\Theta^{(0)} \in \mathbb{R}_+^{MK}$, initial step sizes $\mu_\Theta, \mu_y > 0$ satisfying $0 < \mu_\Theta, \mu_y < \frac{1}{J_h}$, penalty growth factor $\rho > 1$, Armijo parameter $\delta > 0$, tolerance $\zeta > 0$, initial penalty parameter $\chi_1 > 0$, reduction factor $0 < v < 1$.

(2) **initialization:**

$$\Theta^{(1)} = y^{(1)} = \Theta^{(0)}, \qquad g^{(1)} = g^{(0)} = 1,$$

$$d \leftarrow 1, \qquad m \leftarrow 1.$$

(3) Repeat;
Define the penalized objective function:

$$h_{\chi_m}(\Theta) = \frac{u(\Theta)}{v(\Theta)} - \chi_m \sum_{k=1}^{K} \omega_k(\Theta).$$

(4) Repeat
Gradient Projection Step:

$$u^{(d+1)} = K_{\mathcal{C}}\left(y^{(d)} + \mu_y \nabla h_{\chi_m}(y^{(d)})\right),$$

$$v^{(d+1)} = K_{\mathcal{C}}\left(\Theta^{(d)} + \mu_\Theta \nabla h_{\chi_m}(\Theta^{(d)})\right),$$

where $K_{\mathcal{C}}(\cdot)$ denotes projection onto the feasible set $\mathcal{C}$.

(5) **Step Size Update**:

$$s_y^{(d)} = u^{(d)} - y^{(d-1)},$$

$$r_y^{(d)} = \nabla h_{\chi_m}(u^{(d)}) - \nabla h_{\chi_m}(y^{(d-1)}).$$

Update μ_y using either

$$\mu_y = \frac{(s_y^{(d)})^T s_y^{(d)}}{(s_y^{(d)})^T r_y^{(d)}},$$

Similarly,

$$s_\Theta^{(d)} = v^{(d)} - \Theta^{(d-1)},$$

$$r_\Theta^{(d)} = \nabla h_{\chi_m}(v^{(d)}) - \nabla h_{\chi_m}(\Theta^{(d-1)}).$$

Update μ_Θ using either

$$\mu_\Theta = \frac{(s_\Theta^{(d)})^T s_\Theta^{(d)}}{(s_\Theta^{(d)})^T r_\Theta^{(d)}},$$

(6) **Backtracking Line Search for** $u^{(d+1)}$ Repeat

$$u^{(d+1)} = K_{\mathcal{C}}\left(y^{(d)} + \mu_y \nabla h_{\chi_m}(y^{(d)})\right),$$

$$\mu_y \leftarrow v\mu_y.$$

Until

$$h_{\chi_m}(u^{(d+1)}) \geq h_{\chi_m}(y^{(d)}) + \delta\|u^{(d+1)} - y^{(d)}\|^2$$

(7) **Backtracking Line Search for** $v^{(d+1)}$

Repeat

$$v^{(d+1)} = K_{\mathcal{C}}\left(\Theta^{(d)} + \mu_\Theta \nabla h_{\chi_m}(\Theta^{(d)})\right),$$

$$\mu_\Theta \leftarrow v\mu_\Theta.$$

Until

$$h_{\chi_m}(v^{(d+1)}) \geq h_{\chi_m}(\Theta^{(d)}) + \delta\|v^{(d+1)} - \Theta^{(d)}\|^2$$

(8) **Accelerated Proximal Gradient Update**

$$y^{(d)} = \Theta^{(d)} + \frac{g^{(d-1)}}{g^{(d)}}\left(u^{(d)} - \Theta^{(d)}\right) + \frac{g^{(d-1)} - 1}{g^{(d)}}\left(\Theta^{(d)} - \Theta^{(d-1)}\right).$$

If

$$h_{\chi_m}(u^{(d+1)}) \geq h_{\chi_m}(v^{(d+1)})$$

$$\Theta^{(d+1)} = u^{(d+1)}.$$

$$\Theta^{(d+1)} = v^{(d+1)}.$$

(9) Update momentum parameter:

$$g^{(d+1)} = \frac{\sqrt{4(g^{(d)})^2 + 1} + 1}{2}.$$

$$d \leftarrow d + 1.$$

Until

$$\left| \frac{h_{\chi_m}(\Theta^{(d)}) - h_{\chi_m}(\Theta^{(d-10)})}{h_{\chi_m}(\Theta^{(d)})} \right| \leq \zeta$$

(10) **Outer Penalty Update**

$$\Theta^{(1)} = y^{(1)} = \Theta^{(d)},$$

$$\chi_{m+1} = \rho \chi_m,$$

$$m \leftarrow m + 1.$$

(11) until Convergence of the outer penalty loop

(12) **Output:** Optimal solution $\Theta^{\star}$.

3.1.4. Analysis of Convergence for the Penalty-Based APG Method

From the penalized optimization problem in (23), the following assumptions is guaranteed;

(i) The feasible set $\mathcal{C}$ is non empty, closed and convex

(ii) The penalized objective function $h_\chi(\Theta)$ is continuously differentiable.

(iii) The gradient $\nabla h_\chi(\Theta)$ is Lipschitz continuous with constant $J_h > 0$. Thus;

$$||\nabla h_\chi(\Theta_1) - \nabla h_\chi(\Theta_2)|| \leq J_h ||\Theta_1 - \Theta_2|| \quad \forall \Theta_1, \Theta_2 \in \mathcal{C}$$

(iv) The step size satisfies;

$$0 < q\mu_\Theta, \mu_y < \frac{1}{J_h}$$

At every iteration, the algorithm performs a projected gradient ascent step followed by backtracking line search satisfying ;

$$h_{\chi_m}(u^{(d+1)}) \geq h_{\chi_m}(y^{(d)}) + \delta ||u^{(d+1)} - y^{(d)}||^2 \tag{25}$$

and

$$h_{\chi_m}(v^{(d+1)}) \geq h_{\chi_m}(\Theta^{(d)}) + \delta ||v^{(d+1)} - \Theta^{(d)}||^2 \tag{26}$$

Equations (25) and (26) guarantee a sufficient ascent of the penalized objective function during each iteration. Hence, the sequence $h_{\chi_m}(\Theta^d)$ is monotonically non- decreasing . Again, since the feasible set $\mathcal{C}$ is bounded and the penalized objective function is upper bounded over $\mathcal{C}$ [23], the monotone convergence theorem ensures that $h_{\chi_m}(\Theta^d)$ converges to a finite limit. Therefore based on the above assumptions and conditions, the generated sequence converges to a stationary point satisfying the first order optimality condition $0 \in \nabla h_{\chi_m}(\Theta^\star) + N_{\mathcal{C}}(\Theta^\star)$ where $N_{\mathcal{C}}$ is the normal cone of the feasible set $\mathcal{C}$. Furthermore, owing to the Nesterov-type acceleration mechanism in [24] employed in the penalty based APG updates, the algorithm achieves a convergence rate of $\mathcal{O}\left(\frac{1}{d^2}\right)$.

3.1.5. Computational Complexity for the Penalty-Based APG Algorithm

Computational complexity of the proposed penalty-based APG algorithm is dominated by gradient evaluations and projections over the MK- dimensional optimiztion vector. Each inner penalty-based APG algorithm iteration incurs a computational cost of approximately $\mathcal{O}(\mathcal{MK})$, while the overall complexity becomes $\mathcal{O}(D_{out} D_{in} MK)$, where D_{in} and D_{out} are number of inner and outer iterations, respectively.

4. Simulation Results and Discussions

The performance of the proposed penalty-based Accelerated Proximal Gradient (APG) algorithm is evaluated using Monte Carlo simulations over independent channel realizations in a cell-free massive Multiple Input Multiple Output (CF-mMIMO) system. The simulation setup considers a square coverage area where multiple distributed Access Points (APs) jointly serve several users under imperfect channel state information (CSI). The proposed APG-based power allocation algorithm is compared against benchmark optimization methods under identical system configurations and convergence tolerances. All simulations are performed using MATLAB R2024a (The MathWorks, Inc., Natick, MA, USA) on a computer equipped with an Intel Core i7 Processor, 16 GB RAM, Windows 11 Operating System.

4.1. Simulation Parameters

We investigate CF- mMIMO systems, where M access points and K users are evenly and evenly dispersed throughout a (1×1), km^2 area, utilizing the wrap-around technique. The following is the model for the large-scale fading coefficient:

$$\iota_{mk} = KJ_{mk} \cdot z_{mk}, \tag{27}$$

where, z_{mk} = log-normal shadowing having standard deviation σ_{sh} =8 dB, and KJ_{mk} =slope-based pathloss, formulated in dB as follows:

$$KJ_{mk} = -J - 35\log_{10}(d_{mk}), if d_{mk} > d_1,$$

$$KJ_{mk} = -J - 15\log_{10}(d_1) - 20\log_{10}(d_{mk}), if d_0 < d_{mk} \leq d_1,$$

$$KJ_{mk} = -J - 15\log_{10}(d_1) - 20\log_{10}(d_0), if \;\; d_{mk} \leq d_0.$$

Figure 2 plots the energy efficiency of the suggested APG algorithm against the number of iterations while comparing various antenna counts (M = 20, 15, and 10) under sum power constraints at each AP.

Figure 2's graph illustrates how, when the number of iterations is relatively small, the APG method under the cumulative power constraint at each AP has a direct relationship with that number. For this reason, the energy efficiency at each AP increases as the number of repeats increases.

The suggested APG algorithm shows a positive association between energy efficiency and the number of iterations in Figure 2. The inclusion of various antenna numbers (M = 20, M = 15, and M = 10) would typically contribute to higher energy efficiency after establishing the general positive correlation because more antennae meant more degrees of freedom for optimizing signal transmission. In addition, the algorithm moves closer to a steady resolution. The algorithm is approaching an optimal state where making more tweaks has a decreasing effect on energy efficiency, as indicated by the convergence.

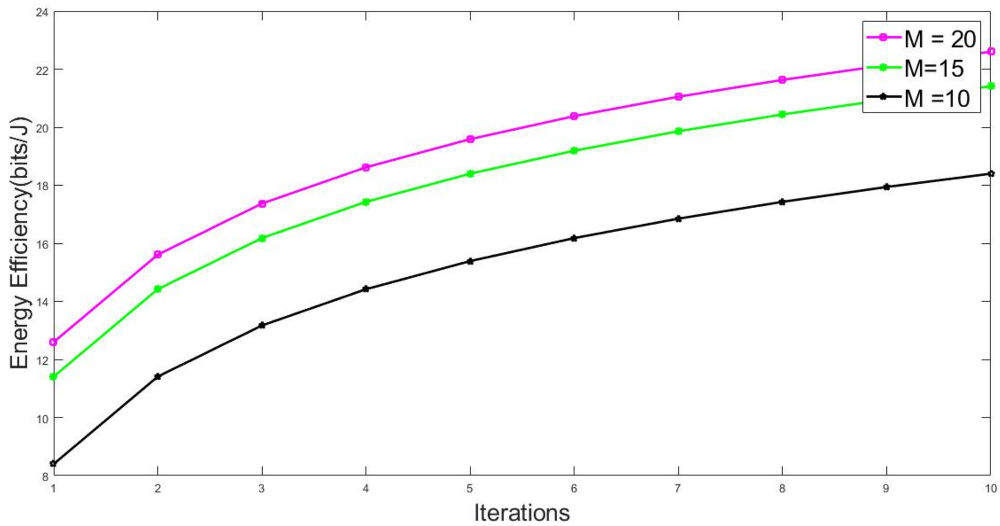

Figure 2. Energy efficiency versus number of iterations.

Figure 3 displays a plot of the proposed APG algorithm's energy efficiency against the number of transmitting antennas and varying minimum attainable rates, all with varying Quality of Service requirements. Figure 3, examines how the proposed APG algorithm's energy efficiency is affected by the Quality of Service (QoS) requirement for M = 10, taking into account varying power allocations for distinct spatial channels. The improvements in energy efficiency with the number of transmitting antennas, as seen in Figure 3. This makes sense given that the system can accommodate more users by making full use of spatial multiplexing. As a result, the system manages to decrease power consumption without compromising system throughput, as illustrated. The effect of Quality of Service (QoS) is seen in Figure 3. In particular, a pattern becomes apparent: instances with higher QoS requirements, denoted by raised values of $R_{m,\text{min}}$, exhibit somewhat lower energy efficiency than do examples with lower QoS requirements. Users are forced to strike a careful balance between maximizing energy economy and achieving their desired minimum data rate, which has important consequences for decision-making.

Moreover, Figure 3 once again imparts valuable insights into determining the optimal number of transmitting antennas that strike a balance between energy efficiency and QoS. Users can determine the optimal energy efficiency point based on their unique quality of service requirements. This information assists clients in making educated decisions regarding transmit antenna arrangement by offering an optimal balance between energy efficiency and meeting the Quality of Service requirements.

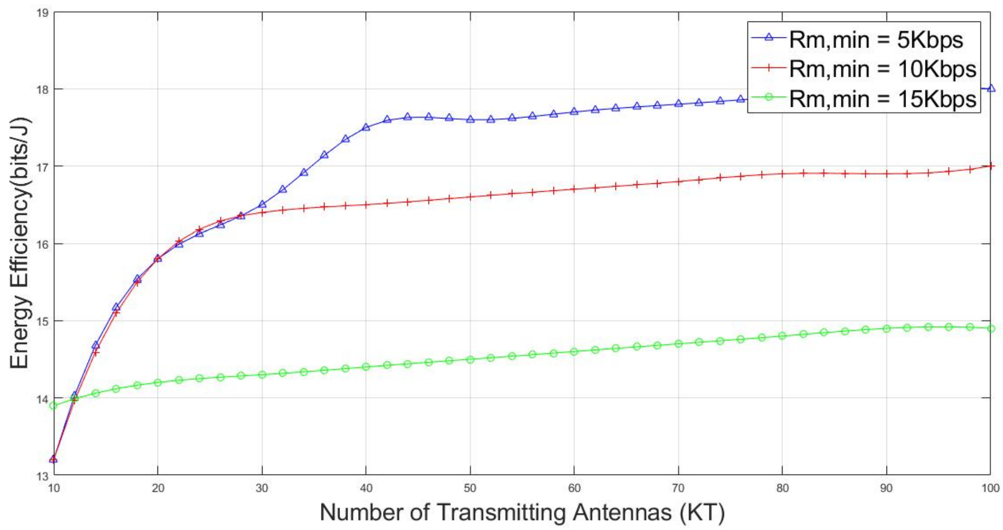

Figure 3. Energy efficiency in relation to antenna count.

Figure 4 compares the spectral efficiency of several algorithms with the total number of users, such as sequential Second Order Cone Programs (SOCPs) and Energy Efficient Equal Power Allocation (EEEPA). Plotting the spectral efficiency in bits/joule against the total number of users, Figure 4 compares the proposed APG algorithm with the Sequential Second-order Cone Program (SOCPs) algorithm in [16] and the Energy Efficient Equal Power Allocation algorithm in [15].

Figure 4 illustrates how the suggested APG algorithm performs better than EEEPA in [15] and Sequential SOCPs in [16]. This is due to the fact that the proposed APG algorithm can distribute optimal power to users based on their individual channel gains, something that Sequential SOCPs and EEEPA cannot do, and as a result, it has a greater spectral efficiency.

Figure 5 compares the overall energy usage of the various algorithms listed in the reference with the maximum transmit power. Figure 5, shows a comparison of a total energy consumption against maximum transmit power among different algorithms. It can be seen that the proposed algorithm (APG algorithm) exhibits a gradual increase in total energy consumption with an increase in maximum transmit power as compared to the Sequential SOCPs in [16] and EEEPA in [15]. Therefore, the proposed algorithm has less energy consumption compared to SOCPs and EEEPA algorithms.

Figure 6 compares a number of power allocation strategies for energy efficiency versus signal-to-noise ratio. Figure 6 shows how energy efficiency increases with SNR for a constant total number of users in the system. This is due to the fact that when SNR rises, the signal's strength relative to noise improves, creating improved channel conditions that allow the system to operate at the same level while using less transmit power.

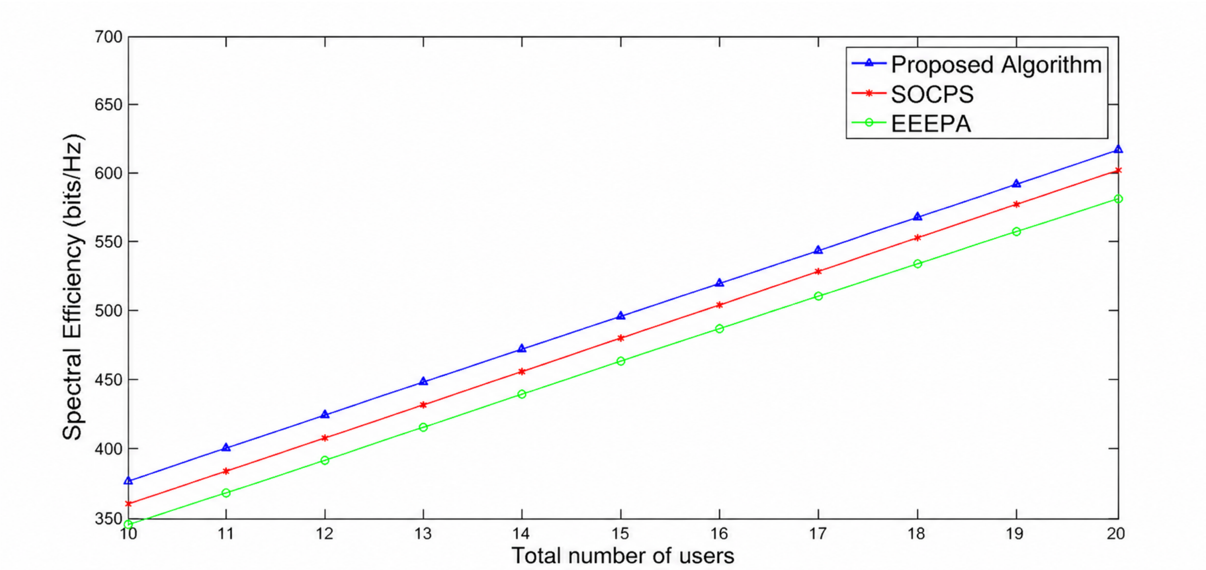

Figure 4. spectral efficiency against the total number of users.

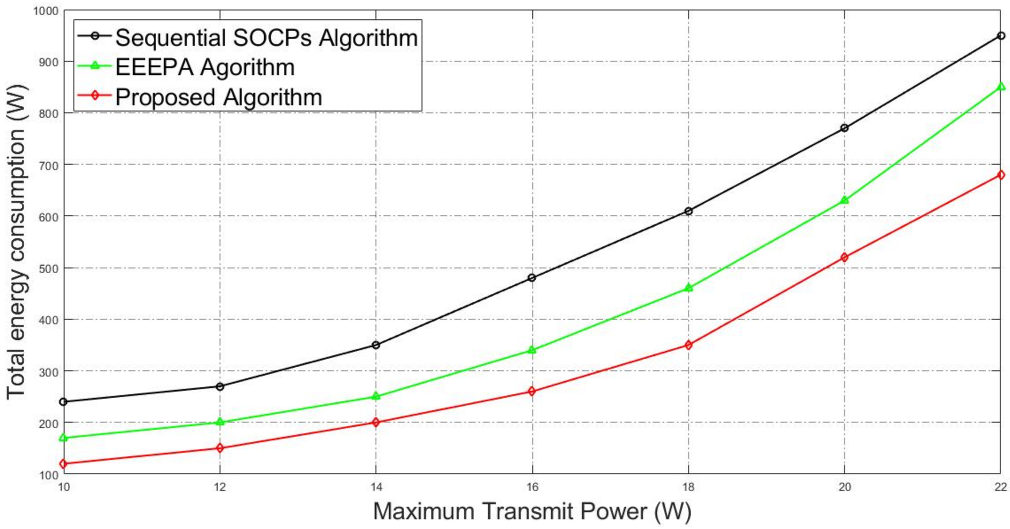

Figure 5. Overall energy use compared to maximum transmit power.

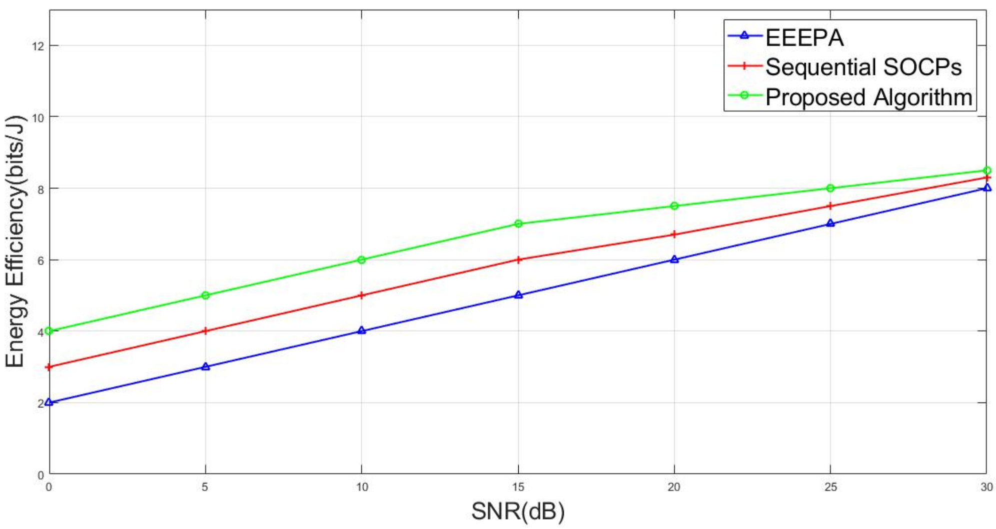

Figure 6. Energy efficiency against SNR.

Figure 7 shows a plot of runtime against the number of APs (M) and users (K). This is done in order to compare the suggested APG algorithm's runtime to the existing algorithm provided in the sources. It is observed from the plot that the proposed APG Algorithm has less execution time compared to SOCPs and EEEPA, as shown in Table 2. Table 2 shows that runtime grows in proportion to the number of access points, however, the suggested approach has a significantly shorter runtime than SOCPs and EEEPA.

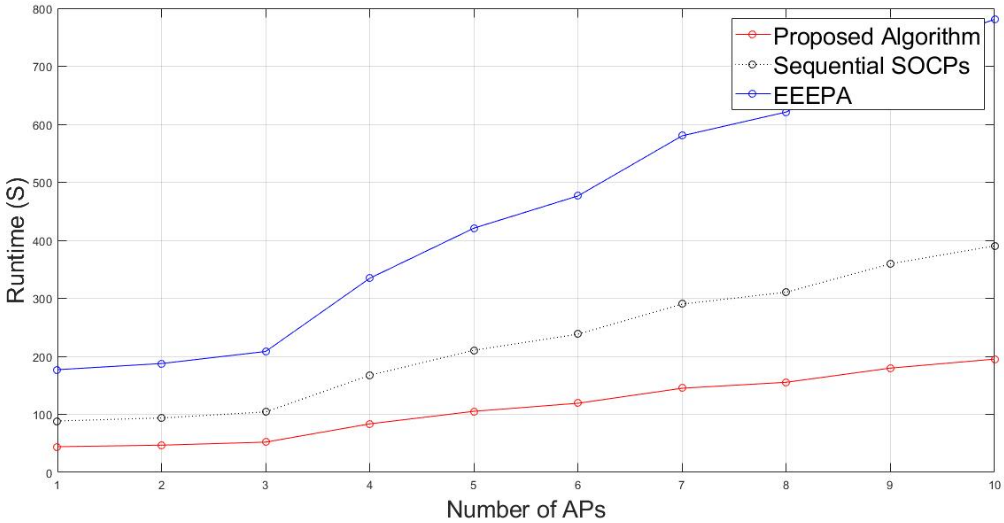

Figure 7. Execution time in relation to the quantity of access points (APs) M.

Table 2. Simulation parameters for power allocation.

Parameter	Symbol	Value
Number of APs	M	50
Number of Users	K	10
Number of Antennas per AP	L	4
Bandwith	B	20 MHz
Coherence interval	τ_c	200 samples
Pilot length	τ_p	10
Downlink transmit power	ρ_d	200 mW
Noise power spectral density	N_0	-174 dBm/Hz
QoS threshold	η_k	1 bps/Hz
AP power budget	P_{max}	1 W
Power amplifier efficiency	ξ	0.4
Circuit power per AP	P_c	0.2 W
Penalty growth factor	ρ	1.5
Initial penalty parameter	χ_1	1
Step size reduction factor	v	0.5
Armijo parameter	δ	10^{-4}
Convergence tolerance	ζ	10^{-5}
Monte Carlo realization		500

Figure 8 illustrates the runtime performance comparison between the proposed penalty-based Accelerated Proximal Gradient (APG) algorithm, the APG algorithm in Reference [18] , Sequential SOCPs, and the EEEPA method as the number of Access Points (APs) increases from 1 to 10.

The results clearly show that the runtime of all algorithms increases with the number of APs due to the higher optimization dimensionality and increased computational burden associated with larger cell-free massive MIMO networks. However, the proposed APG algorithm consistently achieves the lowest runtime across all simulation scenarios.

Specifically, when the number of APs is equal to 1, the proposed APG algorithm requires approximately 45 s, whereas the APG method in Reference [18] requires about 88.5 s. Under the same condition, Sequential SOCPs and EEEPA require approximately 177 s and 388.5 s, respectively. This demonstrates the superior computational efficiency of the proposed framework even for small-scale deployments.

As the number of APs increases to 5, the runtime of the proposed APG algorithm increases moderately to approximately 105.25 s, while the APG algorithm in Reference [18] increases to about 210.5 s. In contrast, Sequential SOCPs and EEEPA exhibit substantially larger execution times of approximately 421 s and 510.5 s, respectively. This indicates that second-order optimization methods incur significantly higher computational overhead compared with the proposed first-order APG framework. At 10 APs, the proposed APG algorithm achieves a runtime of approximately 195.2 s, which remains significantly lower than the runtimes of the benchmark algorithms. Specifically: the APG algorithm in Reference [18] requires approximately 390.4 s, Sequential SOCPs require approximately 780.8 s, while the EEEPA method requires approximately 690.4 s. The results further reveal that the runtime growth of the proposed APG algorithm is nearly linear and considerably more stable than the benchmark schemes (as shown in Table 3).

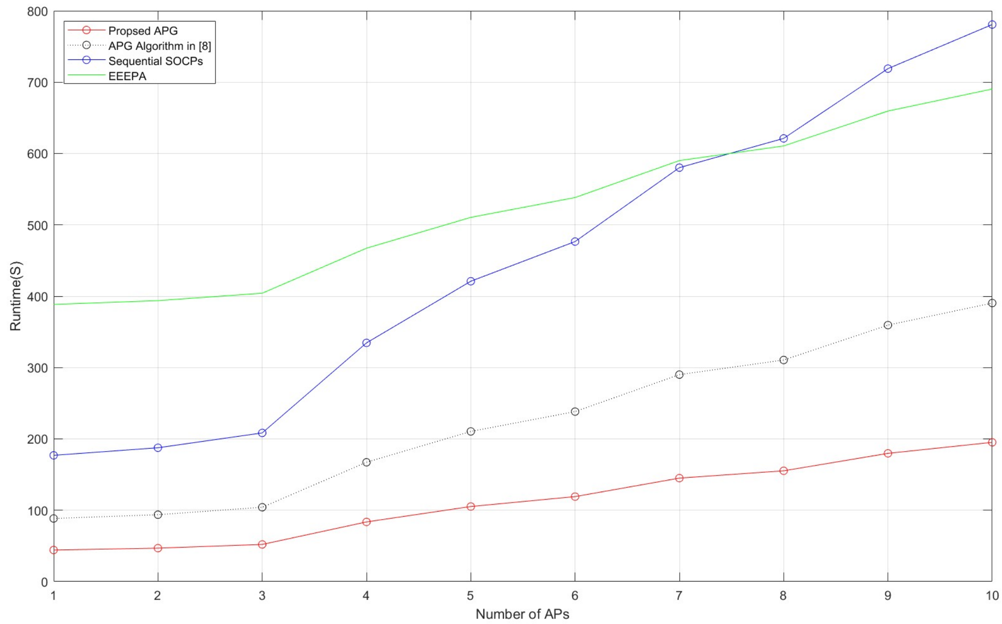

Figure 8. Runtime comparison plot between the proposed APG algorithm verses three benchmark algorithms.

Table 3. Comparison of algorithms with APs, runtimes, and absolute differences in runtime.

Algorithm	Proposed APG Algorithm (A)	SOCPs (B)	EEEPA (C)	$\|B - A\|$	$\|C - A\|$
APs	4	4	4	4	4
Runtime (S)	83.65	167.3	334.6	83.65	250.95
APs	8	8	8	8	8
Runtime (S)	155.3	310.6	621.2	155.3	465.9
APs	10	10	10	10	10
Runtime(S)	195.2	390.4	780.8	195.2	585.6

5. Conclusions

An extensive Energy Efficient optimization challenge in cell-free massive MIMO systems is tackled using the penalty-based APG approach. This entails taking into account the Quality of Service (QoS) limitations at each user as well as the power constraints at the Access Points (APs). The proposed iterative algorithm is then benchmarked against the APG algorithm in [18], the Energy-Efficient Equal Power Allocation (EEEPA) algorithm, and Sequential Second-order Cone Programs (SOCPs) under the specified constraints. The suggested iterative technique, according to the results, produces a higher energy efficiency and a substantially faster runtime, which is shortened by an order of magnitude. This demonstrates how well the method can manage complex optimization problems in cell-free massive MIMO situations found in real-world scenarios. The optimization problem also spans a large-scale fading time scale, meaning that the ideal power control coefficients can only be updated seldom with each large-scale fading realization.

In instances of bursty communication characterized by random user activations, this capability allows for seamless functionality. Lastly, the overall loss will converge to zero since the suggested APG approach won't violate any PFs, regardless of the starting position.

Author Contributions

E.B.B.: developed the concept and conducted a thorough review of existing research, wrote a clear and concise introduction that set the stage for the research, and described the research design and methods; K.A.B.: presented the findings in a clear and organized manner, interpreted the results, related them to existing literature, discussed implications, and summarized the main findings; K.F.D.: ensured the logical flow and organization of the manuscript, and ensured that the writing was clear, concise, and easy to understand; J.A.-M.: created clear and informative tables and figures; J.W.N.: carefully proofread the manuscript for errors and consistencies; K. O.G.: edited the entire work. All authors have read and agreed to the published version of the manuscript.

Funding

This research received no external funding.

Data Availability Statement

Not applicable.

Conflicts of Interest

The authors declare no conflict of interest.

Use of AI and AI-Assisted Technologies

No AI tools were utilized for this paper.

References

1. Zheng, J.; Zhang, J.; Du, H.; et al. Mobile Cell-Free Massive MIMO: Challenges, Solutions, and Future Directions. *IEEE Wireless Commun.* **2024**, *31*, 140–147.
2. Kassam, J.; Castanheira, D.; Silva, A.; et al. A Review on Cell-Free Massive MIMO Systems. *Electronics* **2023**, *12*, 1001.
3. Liu, Y.; Chen, W.; Zhang, J.; et al. Power Allocation for the Fading Relay Channel with Limited Feedback. In Proceedings of the 2010 IEEE International Conference on Communications, Cape Town, South Africa, 23–27 May 2010; pp. 1–5.
4. Pun, M.O.; Porat, R.; Orlik, P.; et al. Codebook-Based Quantized MIMO Feedback for Closed-Loop Transmit Precoding. In Proceedings of the 2009 Conference Record of the Forty-Third Asilomar Conference on Signals, Systems and Computers, Pacific Grove, CA, USA, 1–4 November 2009; pp. 1436–1440.
5. Björnson, E.; Hoydis, J.; Sanguinetti, L.; et al. Massive MIMO Networks: Spectral, Energy, and Hardware Efficiency. *Found. Trends Signal Process.* **2017**, *11*, 154–655.
6. She, F.; Chen, W.; Luo, H.; et al. BER-Based Codebook Construction for MIMO-OFDM Precoded Spatial Multiplexing Systems. In Proceedings of the IEEE GLOBECOM 2007—IEEE Global Telecommunications Conference, Washington, DC, USA, 26–30 November 2007; pp. 3494–3498.
7. She, F.; Chen, W.; Luo, H.; et al. Minimum MSE Based MIMO-OFDM Precoded Spatial Multiplexing Systems with Limited Feedback. In Proceedings of the IEEE GLOBECOM 2007—IEEE Global Telecommunications Conference, Washington, DC, USA, 26–30 November 2007; pp. 3057–3062.
8. He, Y.; Dey, S. Power Allocation in Spectrum Sharing Cognitive Radio Networks with Quantized Channel Information. *IEEE Trans. Commun.* **2011**, *59*, 1644–1656.
9. Zhu, Y.; Fang, Y.; Wang, J. A Partial MRT Algorithm for Closed-Loop Spatial Multiplexing Systems with Transmit Antenna Selection. In Proceedings of the 2006 International Conference on Wireless Communications, Networking and Mobile Computing, Wuhan, China, 22–24 September 2006; pp. 1–4.
10. Sboui, L.; Rezki, Z.; Alouini, M.S. Energy-Efficient Power Allocation for MIMO-SVD Systems. *IEEE Access* **2017**, *5*, 9774–9784.
11. Salh, A.; Audah, L.; Shah, N.M.; et al. Energy-Efficient and Joint Optimal Power Allocation for Distributed Antennas in Massive MIMO Systems. In Proceedings of the 2017 IEEE Asia Pacific Microwave Conference (APMC), Kuala Lumpur, Malaysia, 13–16 November 2017; pp. 881–884.
12. Mosleh, S.; Almosa, H.; Perrins, E.; et al. Downlink Resource Allocation in Cell-Free Massive MIMO Systems. In Proceedings of the 2019 International Conference on Computing, Networking and Communications (ICNC), Honolulu, HI, USA, 18–21 February 2019; pp. 883–887.

13. Bashar, M.; Cumanan, K.; Burr, A.G.; et al. Max–Min Rate of Cell-Free Massive MIMO Uplink with Optimal Uniform Quantization. *IEEE Trans. Commun.* **2019**, *67*, 6796–6815.
14. Bonsu, K.A.; Zhou, W.; Pan, S.; et al. Optimal Power Allocation with Limited Feedback of Channel State Information in Multi-User MIMO Systems. *China Commun.* **2020**, *17*, 163–175.
15. Bonsu, K.A.; Pan, S.; Ansere, J.A.; et al. Joint User Selection and Power Allocation Optimization for Energy-Efficient MU-MIMO Systems with Limited Feedback. *Telecommun. Syst.* **2021**, *77*, 479–492.
16. Björnson, E.; Sanguinetti, L. Scalable Cell-Free Massive MIMO Systems. *IEEE Trans. Commun.* **2020**, *68*, 4247–4261.
17. Dave, S.; Marchisio, A.; Hanif, M.A.; et al. Special Session: Towards an Agile Design Methodology for Efficient, Reliable, and Secure ML Systems. In Proceedings of the 2022 IEEE 40th VLSI Test Symposium (VTS), San Diego, CA, USA, 25–27 April 2022; pp. 1–14.
18. Hao, C.; Vu, T.T.; Ngo, H.Q.; et al. Joint User Association and Power Control for Cell-Free Massive MIMO. *IEEE Internet Things J.* **2024**, *11*, 15823–15841.
19. Kay, S.M. *Fundamentals of Statistical Signal Processing: Estimation Theory*; Prentice-Hall, Inc.: Hoboken, NJ, USA, 1993.
20. Mai, T.C.; Ngo, H.Q.; Egan, M.; et al. Pilot Power Control for Cell-Free Massive MIMO. *IEEE Trans. Veh. Technol.* **2018**, *67*, 11264–11268.
21. Ngo, H.Q.; Tran, L.N.; Duong, T.Q.; et al. On the Total Energy Efficiency of Cell-Free Massive MIMO. *IEEE Trans. Green Commun. Netw.* **2017**, *2*, 25–39.
22. Eriksson, K.; Estep, D.; Johnson, C. Lipschitz Continuity. In *Applied Mathematics: Body and Soul: Volume 1: Derivatives and Geometry in IR3*; Springer: Berlin/Heidelberg, Germany, 2004; pp. 149–164.
23. Vinod, A.P.; Israel, A.; Topcu, U. Constrained, Global Optimization of Unknown Functions with Lipschitz Continuous Gradients. *SIAM J. Optim.* **2022**, *32*, 1239–1264.
24. Van Ngai, H.; Son, T.A. Generalized Nesterov's Accelerated Proximal Gradient Algorithms with Convergence Rate of Order o($1/k^2$). *Comput. Optim. Appl.* **2022**, *83*, 615–649.